Chemical Engineering Science 284 (2024) 119466

Contents lists available at ScienceDirect

Chemical Engineering Science

journal homepage: www.elsevier.com/locate/ces

Chemical recycling of polyethylene terephthalate (PET) to monomers: Mathematical modeling of the transesterification reaction of bis (2-hydroxyethyl) terephthalate to dimethyl terephthalate

Lorenzo Brivio [a,b], Serena Meini [a], Mattia Sponchioni [a,*], Davide Moscatelli [a]

[a] Department of Chemistry, Materials, and Chemical Engineering "Giulio Natta", Politecnico di Milano, Piazza Leonardo da Vinci 32, 20133 Milan, Italy
[b] Whiletrue s.r.l., via Comonte 15, 24068 Seriate, Italy

ARTICLE INFO

Keywords:
Polyethylene terephthalate (PET)
Bis(2-hydroxyethyl) terephthalate (BHET)
Dimethyl terephthalate (DMT)
Transesterification reaction
Kinetic model

ABSTRACT

The accumulation of plastic waste in the environment is making recycling a compelling issue, particularly for polyethylene terephthalate (PET), used in products with a short shelf-life. An appealing route to chemical recycling of PET is glycolysis, leading to bis(2-hydroxyethyl) terephthalate (BHET). Its subsequent transesterification with methanol to dimethyl terephthalate (DMT) is crucial for the recovery of polymer-grade monomers. To favor the industrial applicability of this process, this work investigates the influence of three main parameters, i.e. the methanol to ethylene glycol molar ratio, the solvent to oligomers molar ratio and the mass fraction of the catalyst, on the transesterification of BHET to DMT. A kinetic model has been proposed, and the reaction rates evaluated by comparison with the experimental data. The model was used to predict the performances of the process in a wide range of operating conditions, in order to establish the optimal ones for high yield to DMT.

1. Introduction

Polyethylene terephthalate (PET) is the most common and the cheapest polyester. It has great mechanical, chemical and thermal properties (Mandal and Dey, 2019), and it is mainly employed in the packaging and in the textile industries, accounting for the 8.4 % of the total market share of plastics (PlasticsEurope, 2021). Moreover, the global annual demand for PET, reported to be around 27 million tons in 2022, is expected to reach 42 million tons by 2030 (Statista, 2010). In particular, PET accounts for approximately 54 % of the total production of synthetic fibers (61 million tons in 2021), and for 30 % of all the bottles produced globally (Exchange, 2022). Indeed, PET is mainly used for the manufacturing of products having a very short lifetime (Sinha et al., 2010), which makes it responsible for a huge waste generation. As a matter of fact, PET has the highest ratio between generated waste and production volume among all synthetic polymers (Moscatelli and Pelucchi, 2020).

Thus, apart from replacing PET with novel and more expensive biodegradable plastics, its recycling becomes the only possible way to reduce these huge volumes of waste and, at the same time, to save raw fossil resources and energy (Nikles and Farahat, 2005). Indeed, during the last few decades, the awareness towards environmental pollution caused by uncontrolled plastic waste disposal did sharply increase in the public debate, and nowadays both industries and universities are spending great efforts to find a sustainable solution (Moscatelli and Pelucchi, 2020; Welle, 2011). Lately, the amount of PET bottles which are recycled has increased, but it is still quite low: for instance, only the 26.6 % of the PET bottles sold in the U.S. in 2020 were recycled (PackagingWorld, 2020). The main reasons behind these low numbers are the difficulties in collection, the presence of dyes and plasticizers (which complicate the recycling process), or the fact that the collected waste is usually a blend of PET and other materials that need to be separated in order to allow the recycling of the plastic fraction (Ragaert et al., 2017). Moreover, regarding food-contact PET products, reusing a post-consumer item into another food-contact package is still challenging because of two main reasons: the difficulties in understanding the contaminations of the packaging materials after their recollection, and the poor decontamination efficiency of the state-of-the-art recycling techniques (Welle, 2011; Ghosal and Nayak, 2022).

Moreover, the collected post-consumer PET has broad mechanical properties, chain lengths, and levels of impurities, such that not all the wastes are recyclable. As an example, a technology for recycling PET-

* Corresponding author.
E-mail address: mattia.sponchioni@polimi.it (M. Sponchioni).

https://doi.org/10.1016/j.ces.2023.119466
Received 11 May 2023; Received in revised form 25 October 2023; Accepted 31 October 2023
Available online 2 November 2023

based textiles, which are characterized by poor quality and high difficulties in separating the polyester fraction, is not available at present (Shojaei et al., 2020; Padhan and Sreeram, 2019). Indeed, the 65 % of the total PET produced worldwide in 2020 was landfilled, incinerated, or dispersed, the 25 % was somehow reused, and only the 10 % was actually recycled (MiPol; Gr3n, 2021). Clearly, neither landfilling nor incinerating the PET wastes represent a sustainable solution, and a real recycling technology applicable to all types of wastes is needed to close the loop for PET (Sinha et al., 2010; Barnard et al., 2021).

Currently, PET wastes can be recycled in many ways (Brivio and Tollini, 2022), among which the most efficient are mechanical and chemical recycling. Mechanical recycling is the most diffused technology, but it can only treat the highest quality fraction of PET wastes (i.e., clean and pure bottle flakes). It basically consists in a few well-established steps: washing, shredding into flakes, washing again, drying, and extruding to pellets which can be then post-processed. However, this technique leads to a degradation of the processed waste, such that the obtained material may be inappropriate for the production of food-contact packages (Schyns and Shaver, 2021). Indeed, mechanical recycling is considered a "downcycling" technology, and clearly it cannot be the solution for achieving the goal of a circular economy for PET (Ragaert et al., 2017).

On the other hand, chemical recycling involves the depolymerization of the PET wastes into monomers, their subsequent purification (Geyer et al., 2016; Khoonkari et al., 2015), and a final re-polymerization to yield a polymer having properties and appearance comparable to the virgin material. Thus, only chemical recycling actually allows the "upcycling" of the treated materials, and it can be applied to every kind of PET waste (for instance, both bottle flakes and scrap textiles) (Nikiema and Asiedu, 2022).

Despite these undoubted advantages, the main issue of such a recycling process is the separation and purification of the monomers from the mixture of by-products, solvents, and catalysts used for the depolymerization (Shojaei et al., 2020; Barnard et al., 2021). In fact, PET chemical recycling is usually based on a catalytic reaction conducted in a reactive solvent (usually methanol, ethylene glycol, or water), which is able to cleave the PET ester groups leading to monomers and oligomers. According to the employed reactive solvent, three main methods for performing the PET depolymerization are distinguished: methanolysis, glycolysis, and hydrolysis, leading to dimethyl terephthalate (DMT), bis (2-hydroxyethyl) terephthalate (BHET), and terephthalic acid (TPA), respectively (Sinha et al., 2010). Among these processes, methanolysis and glycolysis are the two most attractive techniques, but besides many advantages, both of them have few drawbacks which are currently limiting their industrial applicability. As an example, methanolysis is more expensive, less flexible, and needs higher temperature and pressure to be performed with respect to glycolysis, but it is more tolerant to lower quality and contaminated feedstocks (Moscatelli and Pelucchi, 2020; Tollini et al., 2022). Moreover, the direct methanolysis of PET textile wastes does not provide satisfactory results in terms of DMT yields, it requires large quantities of cosolvents (i.e., DCM), and it needs very long reaction times (Tollini et al., 2022). On the other hand, the main drawback of glycolysis in the perspective of an industrial applicability is related to the purification of the obtained monomer (BHET), which is quite problematic. Indeed, glycolysis is frequently reported in the literature as a viable method to depolymerize only the cleanest fraction of PET wastes (i.e., clear bottle flakes), obtaining a monomer which is already quite pure and does not need further purification. However, this latter perspective is not industrially attractive since that fraction of PET waste can also be treated mechanically at a much lower cost. On the other hand, chemical recycling becomes attractive when it manages to deal with low quality and contaminated wastes. Thus, in the case studied in this work, the starting PET wastes are represented by mixed and contaminated textiles, such that a monomer purification step becomes necessary and DMT is a much more suitable candidate for such a purification process.

For this reason, two or more PET depolymerization methods could be operated in series to get the advantages and overcome the drawbacks of both (Padhan and Sreeram, 2019). An appealing solution would be, for example, to exploit the milder reaction conditions required by glycolysis to operate the depolymerization first. Then, since BHET is notoriously challenging to purify from the reaction mixture, this could be processed by transesterification with methanol yielding DMT, which can be purified to a polymerization grade monomer (Tomita and Ida, 1973). Indeed, this 2-step approach turns out to allow much higher yields with respect to the direct methanolysis of PET textile wastes, and an easier separation and purification of the final monomer with respect to the glycolysis of such PET textile wastes. This important downstream stage of methanolysis of BHET to DMT, however, is not investigated in the literature. This prevents to draw conclusions about the economic viability of the combined process and, in turn, the rational design of the transesterification reactor.

In order to provide a clear understanding of the kinetics of this transesterification reaction and favor its applicability in an industrial process, in this work we investigated for the first time the influence of 3 main parameters on the final composition of the product mixture: the methanol to ethylene glycol molar ratio (MeOH/EG), the solvent to oligomers molar ratio (Solv/Olig) and the mass fraction of the catalyst (w_{cat}), required to promote the reaction. In particular, among the catalysts that are commonly used to perform transesterification reactions in similar conditions to those employed in this work, *e.g.*, zinc acetate, sodium methoxide, and sodium carbonate, the latter was chosen since it is very cheap and non-toxic, and it ensures very good performances. Moreover, sodium carbonate is an efficient catalyst also for performing the glycolysis of PET, which is intended to be the previous step in the proposed two-stage approach for the chemical recycling of PET textile wastes (i.e., before the BHET to DMT transesterification reaction) (Viana et al., 2011; Sheel and Pant, 2019; Chen et al., 1999; López-Fonseca et al., 2011; Tollini et al., 2022; Pham and Cho, 2021).

A kinetic model of the system was developed and the rate constants for all the involved reactions were determined by comparison with the experimental data collected in a wide design space. The model developed in this work was then exploited to determine the performances of the process in a broad range of operating conditions, and hence to draw conclusions on the most promising set of process parameters aiming at high yields of DMT. It is worth pointing out that this is actually the same reaction but with an opposite goal with respect to what is commonly done in the first step of the polymerization process starting from DMT and yielding BHET (Tomita and Ida; Stratmann, et al., 1992; Jadhav et al., 2020), but the conditions under which the reaction is carried out are too different to allow a direct comparison.

2. Materials and methods

2.1. Materials

Bis(2-hydroxyethyl) terephthalate (BHET, ≥ 94.5 %, Sigma Aldrich), dimethyl terephthalate (DMT, Sigma Aldrich, >99.0 %), 2-hydroxyethyl methyl terephthalate (HEMT, Sigma Aldrich, ≥97 %), terephthalic acid (TPA, Sigma Aldrich ≥ 98 %), methanol (MeOH, ≥ 99.9 %, Sigma Aldrich), ethylene glycol (EG, ≥ 99.8 %, Sigma Aldrich), sodium carbonate (Na_2CO_3, ≥ 99.5 %, Sigma Aldrich), hexafluoro isopropanol (HFIP, ≥ 99 %, Sigma Aldrich), acetonitrile (ACN, ≥ 99.9 %, Sigma Aldrich) were of analytical-grade purity and used as received unless specifically noted.

2.2. Transesterification of BHET to DMT and design of experiments

The transesterification reaction analyzed in this work produces dimethyl terephthalate (DMT) and ethylene glycol (EG) starting from bis (2-hydroxyethyl) terephthalate (BHET) and methanol (MeOH). In particular, this is an equilibrium reaction involving the formation of an

intermediate, namely 2-hydroxyethyl methyl terephthalate (HEMT) (Besnoin et al., 1989). The basic scheme for this reaction is shown in Fig. 1.

The experiments were carried out in a 250 mL three-necked round-bottom flask, equipped with a reflux condenser and a thermocouple, while the third neck was used as a sampling port. The flask was immersed in a pre-heated oil bath in order to keep the reaction temperature constant and equal to 65 °C, and both the oil bath and the system were stirred at 300 rpm by means of a magnetic stirrer to keep the system homogeneous.

In all the trials, the reaction mixture comprised BHET, its oligomers, and methanol as reagents. In addition, ethylene glycol (EG) was added, even if it is a product of the transesterification reaction of BHET to DMT. In fact, this reaction is intended to be operated after the PET glycolysis. Indeed, since glycolysis operates with a slight excess of EG, this is typically found in the product mixture together with BHET (López-Fonseca et al., 2010; Xin, 2021). Thus, the addition of EG allows us to mimic the real glycolysis products which then have to be reacted to yield DMT.

When the reaction temperature reached 65 °C, sodium carbonate (Na_2CO_3) was added as catalyst and its influence on the reaction kinetics was studied. These four compounds (i.e., methanol, ethylene glycol, BHET, and sodium carbonate) were mixed in variable ratios in order to explore a wide spectrum of reaction conditions.

It is important to point out that, since all the mixtures contained a relevant amount of EG, their boiling point were slightly above the boiling point of pure methanol. Indeed 65 °C was chosen as the reaction temperature to avoid boiling for all the reaction mixtures tested and, at the same time, to ensure high reaction rates and improve the productivity.

To perform a systematic and efficient study of this transesterification reaction, a design of experiments (DoE) approach has been adopted, which is an effective tool for maximizing the information gained from a study minimizing at the same time the amount of data to be collected. Instead of varying independently the moles of the four components involved in the reaction, we selected three ratios as factors for the DoE, namely the methanol to ethylene glycol molar ratio (MeOH/EG), the solvent (methanol + ethylene glycol) to oligomers (BHET and its dimer, $BHET_2$, and trimer, $BHET_3$) molar ratio (Solv/Olig) and the mass fraction of the catalyst Na_2CO_3 (w_{cat}). Thus, the different reaction conditions can be represented in a convenient three-dimensional space as shown in Fig. 2.

All the trials were conducted employing a methanol to ethylene glycol molar ratio ranging from 4 to 60, a solvent to oligomers molar ratio ranging from 30 to 400, and a mass fraction of catalyst ranging from 4.16E-5 to 4.16E-4. These conditions were selected to represent, in a broad range, the typical composition of the product mixture from the PET glycolysis, expected to be conducted before this stage of transesterification, and to investigate the influence of the amounts of fresh methanol and catalyst added to the system. A summary of the initial conditions for all the performed experiments is reported in Table 1.

As an example, in trial D, 5.00 g of BHET were mixed in the flask with 50.00 g of methanol and 25.00 g of ethylene glycol (MeOH/EG = 3.87, and Solv/Olig = 99.83) and heated up to the reaction temperature (65 °C). Then, 10.3 mg of the catalyst (w_{cat} = 1.37E-4) were added to the system allowing the reaction to start. To track the evolution of the reaction, samples were withdrawn at predefined times and quenched by cooling in a water/ice bath before characterization of the mixture composition.

2.3. HPLC characterization

With the purpose of tracking the relative concentration of all the species during the reaction, the samples collected from the reactor were analyzed via high-performance liquid chromatography (HPLC).

The separation and quantification of the different species in the samples were operated on an Agilent 1100 HPLC with an UV detector set at 290 nm. The samples were dissolved in hexafluoro isopropanol (HFIP) and separated on a Restek C18 column (250 *4.6 mm, 5 µm pore size). The eluent was a mixture of HPLC-grade acetonitrile (the organic phase), and Millipore water (the aqueous phase). For the first 10 min, the eluent ratio H_2O/ACN was set to 100/0, then the gradient was run from 100/0 to 0/100 in 45 min, and the last 5 min were spent to re-equilibrate the column back to the initial conditions (Espinosa et al., 2000; Fleckenstein and Fleckenstein, 1988). The injection volume was always kept constant at 10 µL.

All the peaks were identified, and the instrument calibrated by injecting standards at known concentrations. Therefore, the monomer concentration was computed by integrating the corresponding peaks after external calibration. As shown in Fig. S1 and Table S1, the UV absorptivity of all the different species was found to be almost equal one to each other. For this reason, the same UV absorptivity found for BHET was used for the quantification of its dimer, $BHET_2$, and trimer, $BHET_3$, as well.

Since all the HPLC analyses were quantitative, the evaluations of parameters such as the BHET conversion (χ_{BHET}) or the DMT yield (η_{DMT}) were computed straightforwardly, according to Equation (1) and Equation (2), respectively, where n_{BHET} are the unreacted moles of BHET, n^0_{BHET} are the initial moles of BHET loaded into the round bottom flask, and n_{DMT} are the moles of DMT which are formed during the

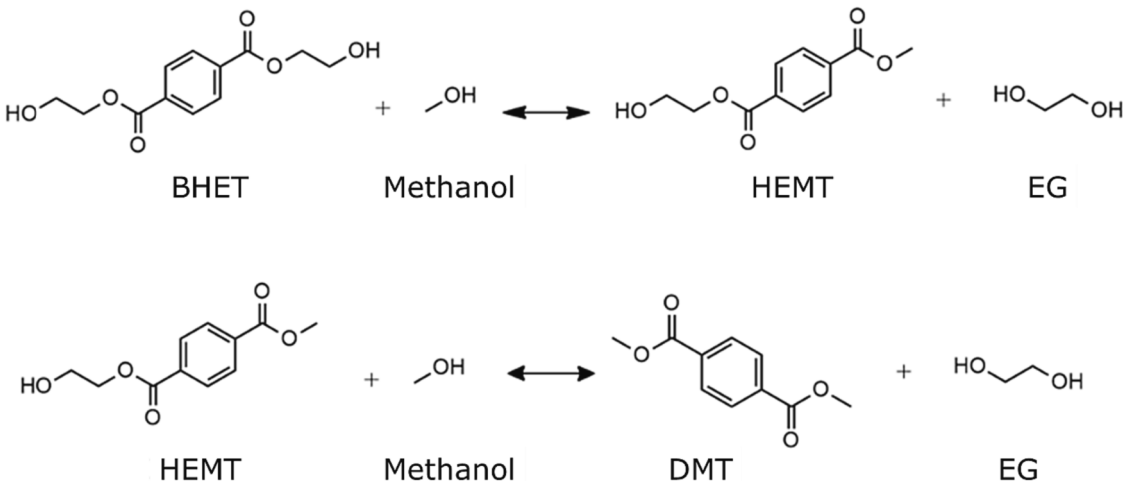

Fig. 1. Transesterification reaction of BHET and methanol to produce DMT and EG.

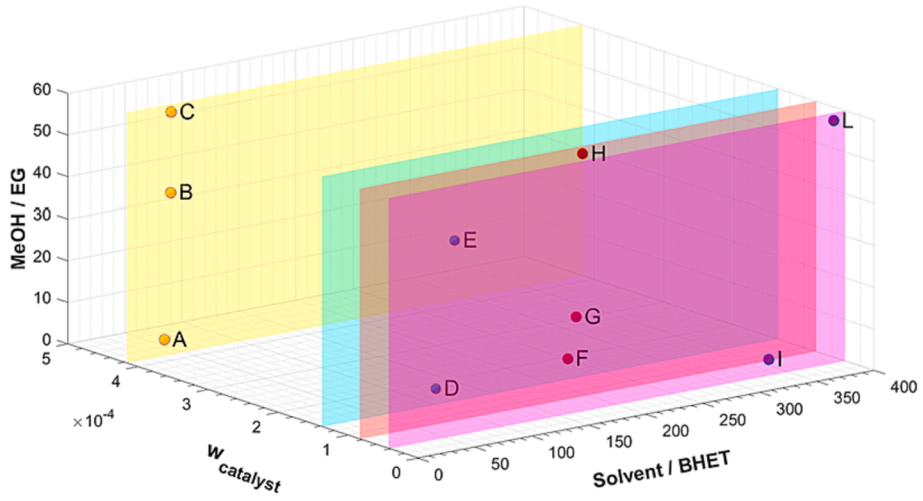

Fig. 2. 3D representation of the entire experimental region for the transesterification reaction. The letters refer to a set of initial conditions explored experimentally, as reported in Table 1.

Table 1
Summary of the performed experiments for the transesterification reaction with the corresponding values of the MeOH/EG ratio, Solvent/oligomers ratio and mass fraction of catalyst. The yield to DMT reached in each experiment at t = 90 min is reported for comparison with the model simulations.

Test name	*MeOH/EG mass ratio*	*MeOH/EG molar ratio*	*Solvent/Olig mass ratio*	*Solvent/Olig molar ratio*	$w_{CATALYST}\left[g_{CAT}/g_{SOLV}\right]$	*DMT yield [-]*
A	2	3.87	5	33.28	4.16 E-4	71.6 %
B	20	38.75	5	38.76	4.16 E-4	91.3 %
C	30	58.12	5	39.06	4.16 E-4	92.1 %
D	2	3.87	15	99.83	1.37 E-4	72.4 %
E	20	38.75	15	116.28	1.37 E-4	94.5 %
F	5	9.69	25	182.38	8.30 E-5	86.7 %
G	10	19.37	25	189.65	8.30 E-5	91.2 %
H	30	58.12	25	195.28	8.30 E-5	96.5 %
I	2	3.87	50	332.77	4.16 E-5	71.2 %
L	30	58.12	50	390.56	4.16 E-5	94.4 %

reaction.

$$\chi_{BHET} = n_{BHET}/n^0_{BHET} \tag{1}$$

$$\eta_{DMT} = n_{DMT}/n^0_{BHET} \tag{2}$$

In particular, the DMT yield was used as the main parameter to evaluate and select the best conditions for carrying out the transesterification reaction from BHET to DMT.

2.4. Optimization algorithm

The values of all the relevant parameters present in the kinetic model of the transesterification reactions were estimated by performing a nonlinear regression using MATLAB®. Indeed, the experimental data were compared with the values simulated by the kinetic model and the sum of the squared errors (SSE) was selected as the objective function to minimize (Chai and Draxler, 2014). The SSE function is reported in Equation (3), where N_{exp} and $N_{species}$ are the number of the experiments and the number of the species, while c_i^{model} and c_i^{exp} are the concentrations of the species predicted by the model and measured experimentally, respectively. It is important to underline that the optimization was performed only on the molar fraction of the oligomers and not on those of EG and MeOH, since it was not possible to measure accurately the variation of such concentrations throughout the reaction.

$$SSE = \sum_{i=1}^{N_{exp}} \sum_{j=1}^{N_{species}} \left(c_i^{model} - c_i^{exp}\right)^2 \tag{3}$$

The minimization of this objective function was performed using the genetic algorithm function coupled with the *fmincon* solver, in order to couple the robustness of the former with the precision of the latter and to be sure the minimum found was actually the global one (El-Mihoub et al., 2006). Then, the Kendall rank correlation coefficient (τ) was used to judge and compare the different optimization results and to find the best one. Indeed, this parameter is a statistic index frequently used to test the non-linear dependences between two variables, which in this case are the reaction time and the mole fractions of the species (Abdi, 2008).

3. Results and discussion

3.1. Characterization of the species involved in the reaction

The composition of the reaction mixture was tracked during time by HPLC, after appropriate external calibration. In particular, the system comprises five species. The feedstock contains the monomer BHET, its dimer ($BHET_2$) and its trimer ($BHET_3$). However, these oligomers are highly reactive, and their characteristic peaks can only be appreciated at the beginning of the reaction (Fig. 3a). Indeed, they disappear in few minutes after the addition of the catalyst, while the characteristic peaks of HEMT and DMT show up (Fig. 3b). As expected, BHET reacts to yield HEMT, which is further converted to DMT, with neither BHET nor HEMT being totally consumed, since these reactions are reversible.

The characteristic retention times of the five species identified during the reaction are reported in Table 2.

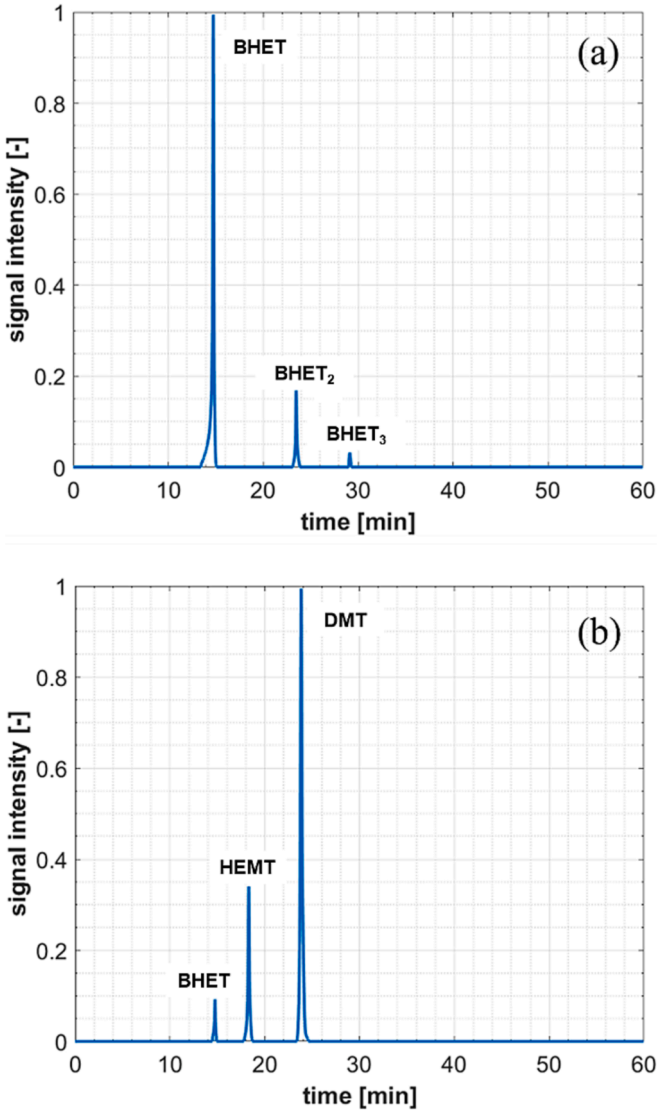

Fig. 3. (a) Chromatogram of the feedstock (t = 0) for the transesterification reaction. (b) Chromatogram of the sample taken during the transesterification reaction at t = 40 min.

Table 2
List of the species involved in the transesterification reaction with their retention times according to the optimized HPLC method (ACN/H2O gradient from 0/100 to 100/0 in 45 min).

Monomer	Retention time [min]
Bis(2-hydroxyethyl) terephthalate (**BHET**)	14.75
2-hydroxyethyl methyl terephthalate (**HEMT**)	18.33
Bis(2-hydroxyethyl) terephthalate dimer (**$BHET_2$**)	23.49
Dimethyl terephthalate (**DMT**)	23.83
Bis(2-hydroxyethyl) terephthalate trimer (**$BHET_3$**)	29.09

3.2. Experimental results and development of the kinetic model

The evolution of the transesterification reaction was systematically investigated at fixed temperature (65 °C) and at different MeOH/EG, Solvent/Olig and w_{cat}. The role of MeOH/EG and w_{cat} is clearly highlighted in Fig. 4, where the evolution of the concentration of all the species involved in the transesterification reaction are reported for four relevant trials (*Test A*, *Test C*, *Test I*, and *Test L* in Table 1*)*. Similar graphs obtained for all the other trials are reported in Fig. S2.

From these preliminary results, it is confirmed that the molar fractions of BHET, $BHET_2$ and $BHET_3$ decrease as the reaction proceeds, but the BHET monomer, unlike the dimer and the trimer, is not entirely consumed. Moreover, two reaction intermediates were detected, whose mole fractions first increase and then decrease. The most relevant one is 2-hydroxyethyl methyl terephthalate (HEMT), while the other one is the dimer of HEMT ($HEMT_2$), which is formed in a very small quantity (<1% mol) and disappears almost instantaneously. Moreover, the latter was not even detected in many of the trials carried out in this work, and due to these reasons, this species was not included in the graphs in Fig. 4 and it was also not considered in the development of the kinetic model. The last species present in the system is the main product of the reaction: DMT, whose molar fraction increases during time. Finally, it is evident that the molar fractions of all the involved species reach a plateau when the equilibrium is reached.

Fig. 4 shows that the molar fraction of DMT at equilibrium is higher as the MeOH/EG molar ratio increases, while the time required to reach the equilibrium seems not much influenced by this parameter. On the other hand, when decreasing the amount of catalyst in the system, the time needed to reach the equilibrium increases (see Fig. S2) while, unsurprisingly, the equilibrium composition of the system does not change at all. Moreover, it is relevant to point out that the reaction does not happen at all when no catalyst is added. Indeed, in the latter case the conversion of BHET (and thus, the yield to DMT) was measured to be 0 % after running the reaction for 90 min. Therefore, the addition of a transesterification catalyst like sodium carbonate is crucial, and due to this observation, the contribution of the un-catalyzed reaction was not considered in the proposed kinetic model.

Based on these experimental observations, the kinetic scheme represented in Fig. 5 was proposed.

It is assumed that only the main reactions occurring in the system (i.e. from BHET to HEMT and from HEMT to DMT) are equilibrium reactions, while for the other ones (i.e., the depolymerization reactions from oligomers to monomers or smaller oligomers) only the direct reaction was considered. Indeed, these oligomeric species had never been detected as intermediates and they are only consumed during the reaction. Moreover, these oligomerizations are not reported at all at the mild operating conditions (i.e., 65 °C, 1 bar) employed in this study (Lin and Baliga, 1986). Therefore, the eight reactions in Fig. 5 are enough to fully describe the evolution of the concentration of the seven different species present in the system, namely BHET, $BHET_2$, $BHET_3$, HEMT, DMT, MeOH and EG.

Since all the experiments were carried out in an isothermal and well stirred batch reactor, the mass balance equation used for a generic species *i* is reported in Equation (4), where n_i is the number of moles of the generic species, V is the reactor volume, r_j is the rate of the generic reaction *j* expressed in $[mol/L/min]$, and $\nu_{i,j}$ is the stoichiometric coefficient of the species *i* in the reaction *j*. The volume was not assumed as constant since in principle it can vary during the reaction, as ethylene glycol has a much higher density than methanol. Indeed, the total reaction volume was computed as the sum of the volumes of all the species, which were calculated at every step of the integration, as shown in Equation (5), where MW_i and rho_i are the molecular weight (expressed in $[g/mol]$) and the density (expressed in $[g/L]$) of the species *i*, respectively. On the other hand, the influence of the withdrawn samples on the total reaction volume was not considered in the development of the kinetic model since the total withdrawn volume accounted for less than 0.9 % of the total reaction volume.

$$\frac{dn_i}{dt} = \sum_j \nu_{i,j} r_j V \tag{4}$$

$$V_i = \frac{n_i MW_i}{rho_i}$$

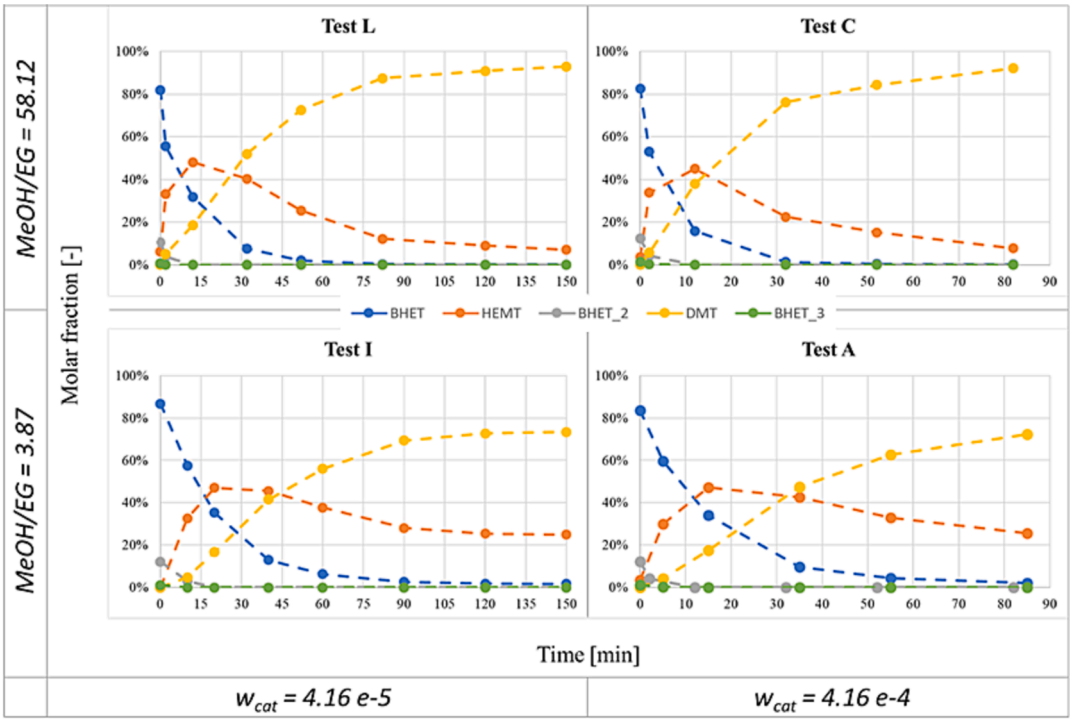

Fig. 4. Concentration of the five species involved in the transesterification reaction of BHET to DMT during time by varying the MeOH/EG and w_{cat} for trial L, C, I, and A reported in Table 1.

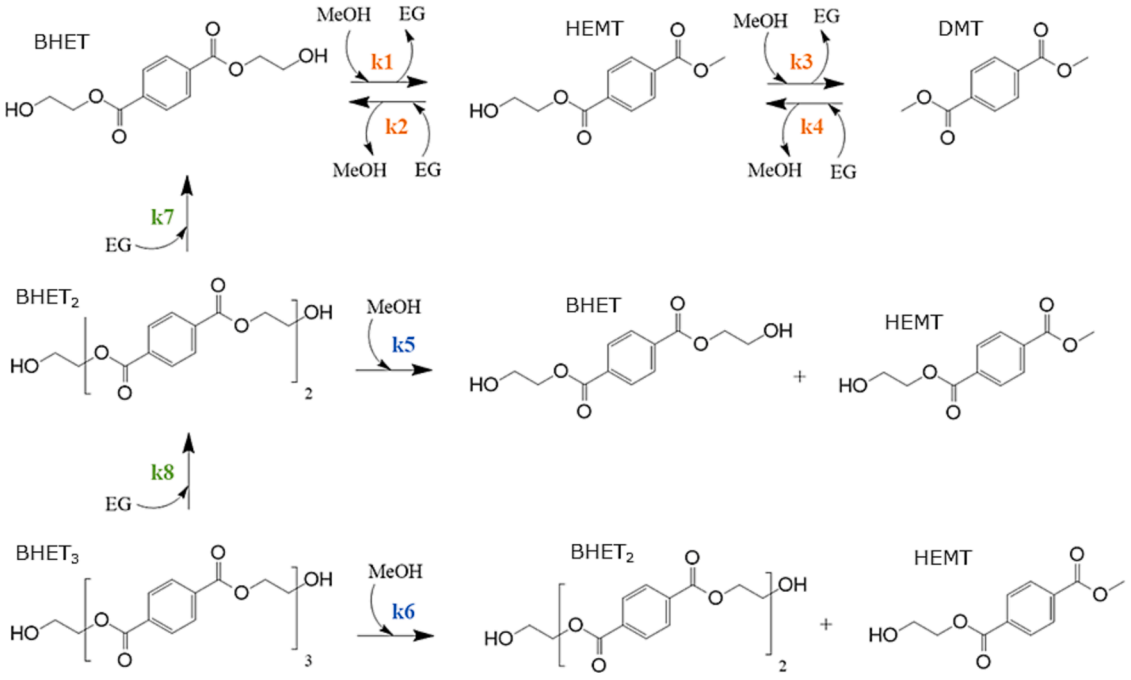

Fig. 5. Kinetic scheme of the BHET to DMT transesterification reaction.

$$V = \sum_{i=1}^{NS} V_i \tag{5}$$

For the sake of completeness, the material balances for all the species involved in the system are reported in Equation S1.

All the eight reactions were treated as elementary reactions, and a reaction order equal to one has been considered for all the species. The expression of the eight reaction rates is reported in Equation (6), where the kinetic constants are expressed in $[L/mol/min]$, and all the kinetic constants are expressed as the probability of bond formation or bond breakage.

$$r_1 = k_1 n_{BHET} n_{MeOH} \frac{1}{V^2}$$

$$r_2 = k_2 n_{MHET} n_{EG} \frac{1}{V^2}$$

$$r_3 = k_3 n_{MHET} n_{MeOH} \frac{1}{V^2}$$

$$r_4 = k_4 n_{DMT} n_{EG} \frac{1}{V^2}$$

$$r_5 = k_5 n_{BHET_2} n_{MeOH} \frac{1}{V^2}$$

$$r_6 = 2 \bullet k_6 n_{BHET_3} n_{MeOH} \frac{1}{V^2}$$

$$r_7 = k_7 n_{BHET_2} n_{EG} \frac{1}{V^2}$$

$$r_8 = 2 \bullet k_8 n_{BHET_3} n_{EG} \frac{1}{V^2} \quad (6)$$

Finally, to account for the influence of the catalyst concentration in the system, a dependency of the rate constants from w_{cat} was introduced. In particular, the apparent kinetic constants (k_j) for the generic reaction j are expressed as the product of the intrinsic kinetic constant (k_j') and the mass fraction of catalyst at a reaction order α_j, according to Equation (7), where the mass fraction of catalyst is calculated as reported in Equation (8). All these parameters (i.e., k_j' and α_j) were determined employing the described optimization procedure.

$$k_j = k_j' \bullet w_{CAT}{}^{\alpha_j} \quad (7)$$

$$w_{CAT} = \frac{m_{CATALYST}}{m_{SOLVENT}} \quad (8)$$

3.3. Optimization results and determination of the kinetic constants

The optimization problem comprises 16 parameters, 8 different k_j' and 8 α_j, one pair of parameters for each reaction. These were estimated by minimization of the SSE (Equation (3)) between the concentrations of the different species measured experimentally and those predicted by the model for all the reaction conditions. The possibility of obtaining a good set of parameters, allowing to reproduce the experimental results for the different conditions is testified by Fig. 6, and by a Kendall coefficient equal to 0.92. Then, the numerical values of the 16 optimized parameters are reported in Table 3.

Clearly, the values of α_j for all the transesterification reactions (reactions (1)–(4)) are very similar one to each other (i.e., close to 0.5). On the other hand, the reaction orders α_j for the depolymerizations (i.e., α_5, α_6,α_7,α_8) deviate significantly. In addition, the optimization algorithm is not much stable for the latter values of α_j as shown in Table S2, where the values of the eight α_j from two independent optimization runs are reported. This is ascribed to the high reactivity of the BHET oligomers, and their quick consumption during time, which makes the determination of their actual concentration arduous. Given these considerations, the optimization problem can be simplified in favor of improved robustness and decreased computational time.

At first, according to the type of reaction and to the reactant involved, the 8 reactions were differentiated in 4 groups, and each of them was characterized by a different value for the parameter α (i.e., 4 different values for this parameter were adopted). In particular, the same catalyst reaction order $\alpha_{1,3}$, was attributed to the two transesterification reactions with MeOH (r_1 and r_3), and a different reaction order $\alpha_{2,4}$ was attributed to the two transesterifications with EG (r_2 and r_4). Similarly, an order $\alpha_{5,6}$ was attributed to the two depolymerization reactions with MeOH (r_5 and r_6), and another order $\alpha_{7,8}$ was attributed to the two depolymerizations with EG (r_7 and r_8). In this case, the number of parameters is reduced to 12, including 8 intrinsic rate constants k_j' and 4 reaction orders α_j. The optimization results obtained with this model simplification are reported in Fig. S3 and Table S3. This model did behave in the exact same way as the previous one, as it is also clear from comparing the Kendall coefficients of the two cases. Moreover, from Table S3, it is also confirmed that all the transesterification reactions are characterized by very similar values of α, while the depolymerization reactions behave differently when the species involved are methanol or ethylene glycol.

Therefore, only three different reaction orders α_j were considered in the final optimization problem: one for the insertion of methanol in the depolymerization reactions (r_5 and r_6), one for the insertion of ethylene glycol in the depolymerization reactions (r_7 and r_8), and a last one for all the transesterification reactions (r_1, r_2, r_3, and r_4). Indeed, as already pointed out, there are no significant differences between methanol and ethylene glycol insertion in these equilibrium transesterification reactions, as testified by similar α_j determined so far. The optimization results of the final kinetic model with 11 parameters (i.e., 8 values for the k_j', and 3 values for the α_j) are reported in Fig. 7. This final optimization led to a Kendall coefficient of 0.93, which confirms the good agreement between the experimental data and the model results. The optimized values of all the 11 optimized parameters are reported in Table 4. Moreover, in the latter case the optimization algorithm is very

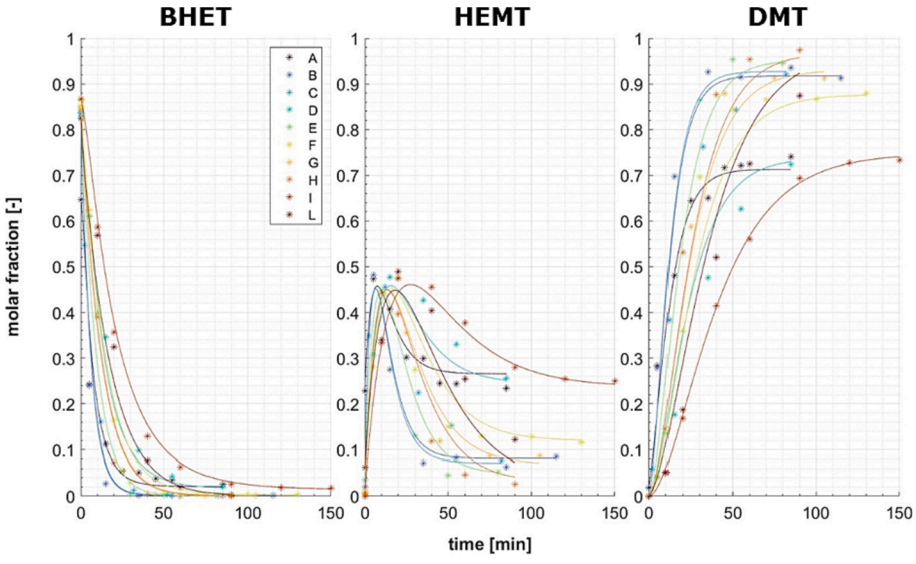

Fig. 6. Optimization results considering eight different values of α.

Table 3
Results of the optimization considering 16 parameters in the kinetic model. $k_j^{'}$ is given in [L/mol/min].

$k_1^{'}$	$k_2^{'}$	$k_3^{'}$	$k_4^{'}$	$k_5^{'}$	$k_6^{'}$	$k_7^{'}$	$k_8^{'}$
0.4590	0.1156	0.3332	0.3035	12.2237	55.3623	3.6284	2.6093
α_1	α_2	α_3	α_4	α_5	α_6	α_7	α_8
0.5110	0.5178	0.5231	0.4954	0.8248	0.8036	0.4169	0.7681

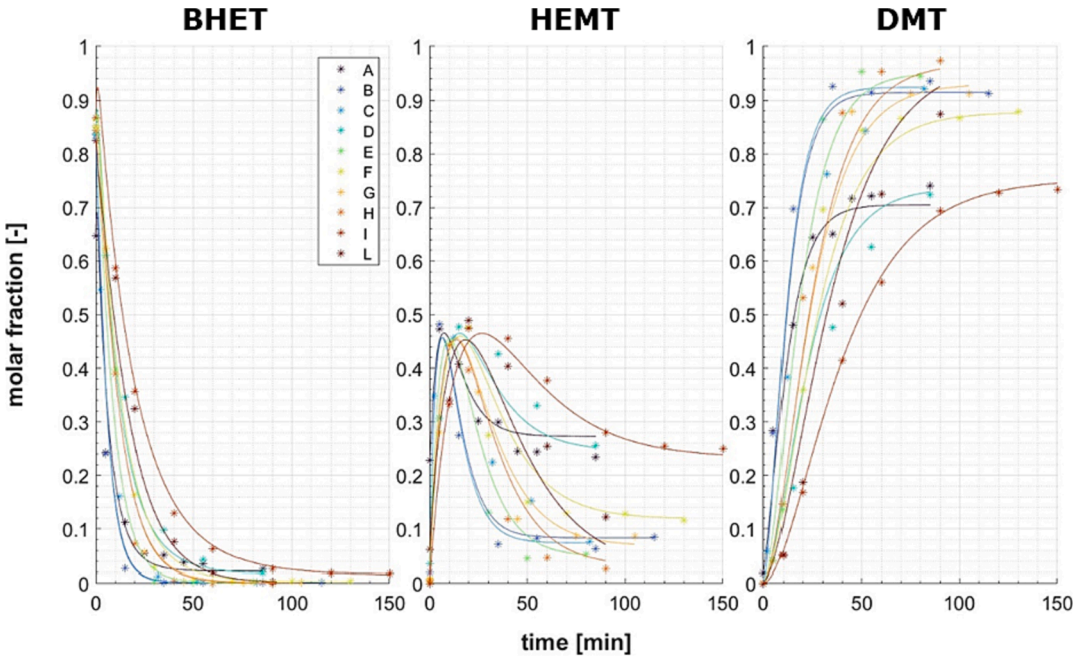

Fig. 7. Optimization results considering three different values of α.

Table 4
Results of the optimization considering 11 parameters in the kinetic model.

$k_1^{'}$	$k_2^{'}$	$k_3^{'}$	$k_4^{'}$	$k_5^{'}$	$k_6^{'}$	$k_7^{'}$	$k_8^{'}$
0.5449	0.1328	0.3412	0.3995	7.4656	19.7110	6.0132	4.6228
	$\alpha_{Trans(1,2,3,4)}$		$\alpha_{DepMeOH(5,6)}$			$\alpha_{DepEG(7,8)}$	
	0.5260		0.7953			0.2896	

stable regarding the values of the parameters α_j. Indeed, as it is shown in Table S4, the three values of α_j found from three independent optimization runs performed by changing the initial guesses turned out to be very similar one to each other.

For the sake of completeness, the evolution of the molar fractions of the BHET dimer and trimer (i.e., $BHET_2$ and $BHET_3$) is reported in Fig. S4, and it has to be highlighted that the consumption of these species is extremely fast, and the influence of these species on the global system is not very relevant. Moreover, in Fig. S5, the experimental DMT yield is plotted and compared to the DMT yield predicted by the model, showing a good reproduction of the experimental behavior for all the conditions of Table 1.

After having defined a good set of kinetic parameters, the model predictivity was validated by simulating an additional set of 4 experiments not used for regression of the kinetic constants. The operating conditions of these 4 reactions in terms of MeOH/EG, Solv/Olig, and w_{cat} were selected in order to validate the model exploring new regions inside the 3D domain represented in Fig. 2, and they are reported in Table 5.

These trials confirm that the model can well predict the evolution of the transesterification reaction also for these new conditions, as shown in Fig. S6. Indeed, the Kendall coefficient for this simulation is equal to 0.89. Therefore, the last 4 experiments validate and confirm the good performances of the kinetic model when the transesterification reaction

Table 5
Summary of the performed experiments for model validation with the corresponding values of the MeOH/EG ratio, Solvent/oligomers ratio and mass fraction of catalyst. The yield to DMT reached in each experiment at t = 90 min is reported for comparison with the model simulations.

Test name	*MeOH/EG molar ratio*	*Solvent/Olig molar ratio*	$w_{CATALYST}\left[g_{CAT}/g_{SOLV}\right]$	*DMT exp. yield [%]*	*DMT mod. yield [%]*	*difference [%]*
M	19.37	113.82	1.37 E-4	91.5 %	93.1 %	1.73 %
N	38.75	193.87	8.30 E-5	94.6 %	96.2 %	1.68 %
O	3.87	166.43	8.30 E-5	71.7 %	72.7 %	1.39 %
P	19.37	379.47	4.16 E-5	88.5 %	88.7 %	0.23 %

is performed inside the 3D domain shown in Fig. 2.

3.4. Model predictions in the full 3D domain

A good agreement between the proposed kinetic model and the experimental data collected at different reaction conditions was demonstrated, and this model was then exploited to predict the reaction behavior in the whole three-dimensional domain shown in Fig. 2. In particular, the main focus was the determination of the role of MeOH/EG, Solv/Olig and w_{cat} on the yield to DMT, which is the main product of this process.

First, only one out of the three parameters was independently varied, while keeping the remaining two constant.

The yield to DMT as a function of the mass fraction of the catalyst (in a range from 10^{-6} to 10^{-3}) and time is shown in Fig. 8a for a reaction time up to 150 min, where MeOH/EG and Solv/Olig were fixed to 25 and 200, respectively. In particular, the latter values ensure that: a) the system operates in excess of methanol, shifting the reaction equilibrium to the product (i.e., DMT), b) the monomers are well dissolved inside the reaction mixture, preserving homogeneous conditions throughout the process. Clearly, the higher the mass fraction of catalyst, the faster the growth of DMT yield up to the equilibrium value. This can be explained with a larger availability of binding sites for the reactants to form the intermediate species for the reaction to proceed, which in turn causes a faster approach to the equilibrium. As a matter of fact, we demonstrated that the rate constants for all the reactions in the kinetic scheme reported in Fig. 5 show a direct proportionality with the catalyst amount.

As an example, if the reaction is performed using a mass fraction of catalyst equal to $1 \bullet 10^{-4}$, 140 min are enough to reach a yield of DMT equal to 94 %, which is practically the equilibrium yield for these operating conditions and is not affected by w_{cat}, as expected. On the other hand, if the mass fraction of catalyst is reduced below $1 \bullet 10^{-5}$, this equilibrium yield is not reached in the timeframe investigated.

The dependence of the DMT yield from MeOH/EG was then studied in the range 1 – 34, keeping constant w_{cat} and Solv/Olig to $2 \bullet 10^{-4}$ and 200, respectively. Again, the latter ensures homogeneous reaction conditions, while the mass fraction of catalyst was set in order to reach equilibrium condition inside the investigated timeframe (150 min). The results of this second set of simulations are shown in Fig. 8b. It turns out that the reaction kinetic is not much affected by the MeOH/EG ratio. In fact, at different MeOH/EG the reaction proceeds at the same rate until the thermodynamic equilibrium is reached (represented in the graph as a light blue vertical line). This is confirmed by the *iso*-yield lines being vertical before approaching the equilibrium conditions. Conversely, the value of the DMT yield at equilibrium does strongly depend on the MeOH/EG molar ratio, because the studied transesterification is an equilibrium reaction and EG and methanol are the products of the direct and inverse reaction, respectively. Indeed, higher yields to DMT are obtained for higher values of the MeOH/EG molar ratio, and when the EG is present in lower amount or it is even not present, the equilibrium is pushed to the product DMT. On the contrary, the presence of higher quantities of EG in the reaction mixture will result in a decrease of the DMT yield. In particular, after 140 min, a MeOH/EG molar ratio of 32 is required in order to achieve a yield of DMT equal to 95 %, while if a 93 % DMT yield is considered sufficient, a MeOH/EG molar ratio of 20 is enough. This consideration drives the selection of the EG excess to be used in the preliminary PET glycolysis, as its residual amount strongly influences the equilibrium of the transesterification from BHET to DMT.

Finally, also the influence of the last parameter, which is Solv/Olig molar ratio, has been investigated in the range 1 – 250, while keeping constant the MeOH/EG equal to 25, and the w_{cat} equal to $2 \bullet 10^{-4}$. The results of these last simulations are shown in Fig. 8c. In the studied conditions, it is evident that the influence of the Solv/Olig molar ratio on the system is minimal. Indeed, the dashed lines on the graph indicating *iso*-yield to DMT are almost vertical and become horizontal only for very low values of the Solv/Olig. In fact, carrying out the transesterification reaction for such low values of Solv/Olig (i.e. < 40, represented by the horizontal red line in the graph), it is not possible to preserve homogeneous conditions during the reaction, and some of the produced DMT does precipitate. This was both experimentally observed and verified by checking the solubilities of BHET and DMT in both MeOH and EG (Huang et al., 2021; Zhang et al., 2013).

It is important to point out that, even if a continuous precipitation of DMT would lead to an easier separation of the monomer and to a lower organic solvent consumption, in the perspective of performing such transesterification reaction after PET glycolysis, a large quantity of methanol has to be employed in order to extract all the BHET from the residual non-depolymerized products, such that the transesterification reaction is likely to be operated in excess of methanol (thus, in homogeneous conditions). Moreover, if the amount of solvent is too small, even the small quantity of EG produced during the reaction can lead to a significant variation of the MeOH/EG molar ratio present throughout the reaction, and this kind of graph loses all its significance. Therefore, it has to be pointed out that the model was not developed to predict the behavior of the transesterification reaction at values of Solv/Olig < 40, and the predictions obtained from the model in this region are not as robust as the ones obtained above the threshold value of Solv/Olig $= 40$. In this region, the EG produced during the reaction has a minimal effect in changing the MeOH/EG molar ratio, since the solvent is present in large excess. Once the equilibrium is reached, the dashed lines become flat also in the region above the threshold value of Solv/Olig $= 40$, and an increase in the DMT yield can be observed also when the solvent to oligomer molar ratio increases, but these changes are minimal. This may be due to the fact that the little amount of EG produced during the reaction is less influential on the actual MeOH/EG molar ratio present throughout the reaction if the Solv/Olig molar ratio is high. For example, if the solvent to oligomers molar ratio is increased from 50 to 180 for a reaction time equal to 140 min, the yield of DMT increases only by 5 % (it passes from 86 % to 91 %).

After having analyzed the effect of changing a single parameter on the DMT yield, the mutual influence of two of these parameters was investigated, while fixing the third one. The results in terms of yield to DMT reached after 90 min are shown in Fig. 9 and these model predictions can be directly compared to the experimental data at the same reaction time, reported in Table 1. Furthermore, the predicted DMT yield over time for the different combinations of process parameters is shown in Figs. S7, S8, and S9.

First, MeOH/EG and w_{cat} were independently varied, while keeping the Solv/Olig molar ratio constant and equal to 200. The first parameter was ranged from 1 to 35, while the second one was ranged from 10^{-6} to 10^{-3}. The results are reported in Fig. 9a. Once again, it is confirmed that the reaction kinetics depends mainly from the mass fraction of catalyst present in the system. Indeed, the dashed lines representing equal yield to DMT are vertical before the equilibrium condition is reached. This indicates that the yield of DMT reached at 90 min increases only with w_{cat}, independently upon the MeOH/EG molar ratio. In particular, if the mass fraction of catalyst is increased, the system reaches higher yields until the limit imposed by the thermodynamic equilibrium, represented by horizontal lines in this plot. These horizontal lines confirm that the equilibrium is not affected by w_{cat}. As a matter of fact, a further increase in w_{cat} above 10^{-4} has no influence on the yield to DMT, which is only affected by MeOH/EG molar ratio. In fact, higher equilibrium yields to DMT can be achieved only by increasing the excess of MeOH. For example, after 90 min, an equilibrium DMT yield equal to 95 % can be obtained operating at MeOH/EG equal to 32, while a molar ratio equal to 18 is enough to reach an equilibrium DMT equal to 92 % after the same reaction time.

Then, the combined effect of both MeOH/EG and Solv/Olig has been studied, in a range from 1 to 40 and from 1 to 200, respectively. The mass fraction of catalyst, instead, was kept constant to $2 \bullet 10^{-5}$. The

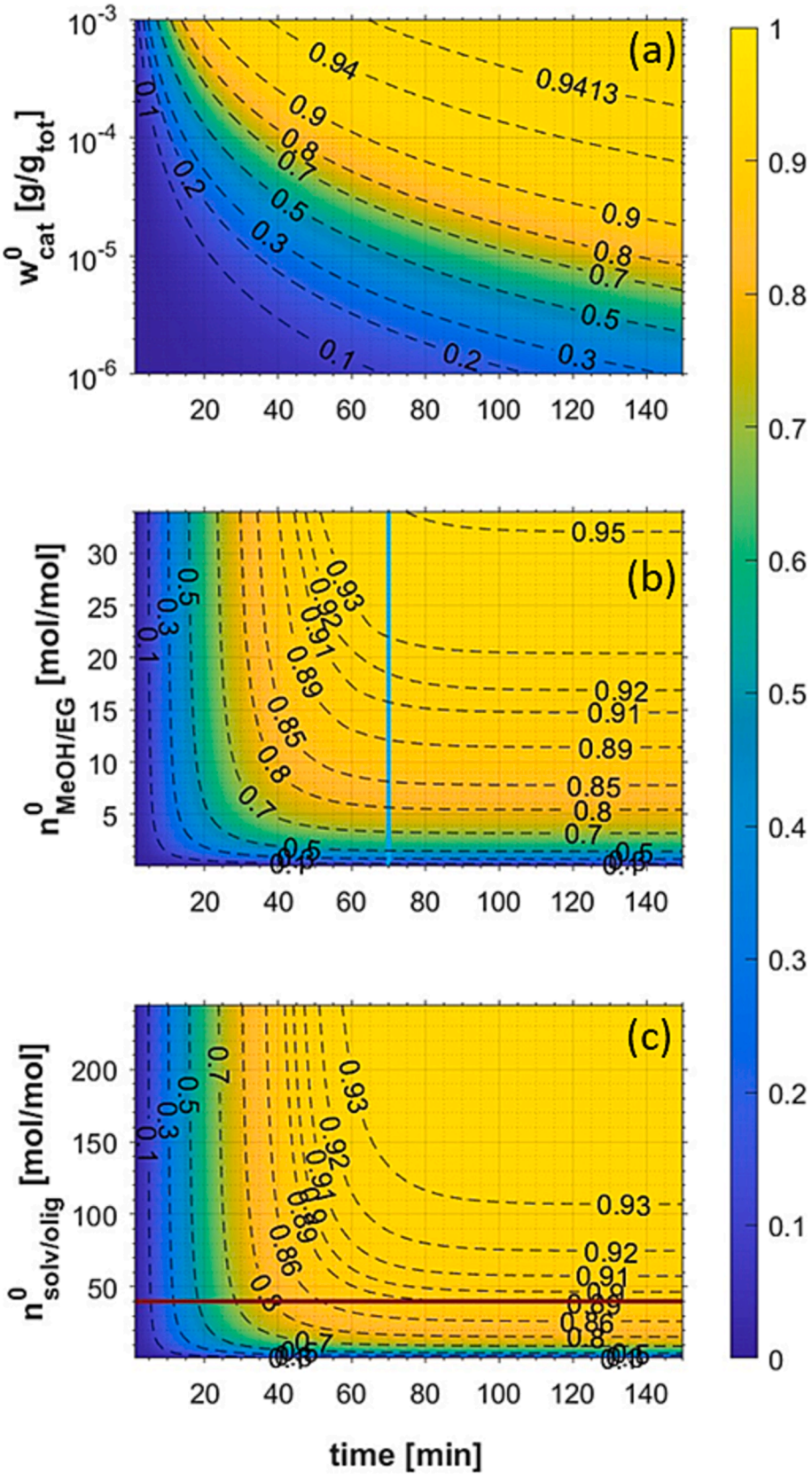

Fig. 8. DMT yield at increasing reaction time by changing: (a) the mass fraction of catalyst, with MeOH/EG and Solv/Olig fixed to 25 and 200, respectively; (b) the methanol to ethylene glycol molar ratio, with w_{cat} and Solv/Olig fixed to $2 \bullet 10^{-4}$ and 200, respectively; (c) the solvent to oligomers molar ratio, with MeOH/EG and w_{cat} fixed to 25 and $2 \bullet 10^{-4}$, respectively.

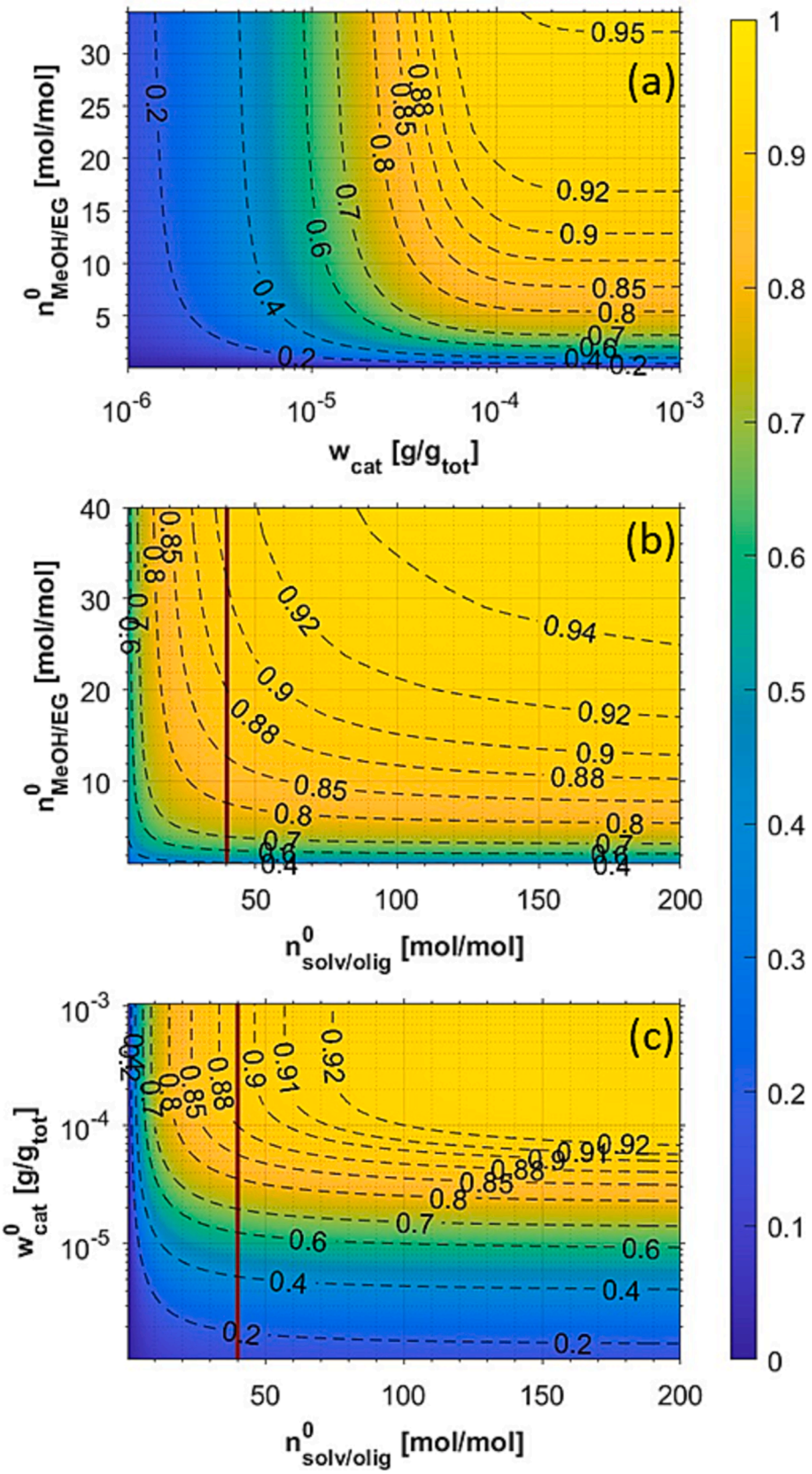

Fig. 9. DMT yield at 90 min by changing: (a) the methanol to ethylene glycol molar ratio and the mass fraction of catalyst (at Solv/Olig = 200); (b) the methanol to ethylene glycol molar ratio and the solvent to oligomers molar ratio (at $w_{cat} = 2{\cdot}10^5$); (c) the solvent to oligomers molar ratio and the mass fraction of catalyst (at MeOH/EG = 16).

results of these simulations in terms of DMT yield are reported in Fig. 9b, where the model predictions have been displayed at t = 90 min. As it was done previously, a red straight line is drawn to highlight the region where the model predictions are more trustworthy (i.e., when Solv/Olig > 40), since homogenous reaction conditions are maintained throughout the whole reaction. In this region it is confirmed that Solv/Olig has a limited effect on the DMT yield, as confirmed by the *iso*-yield lines being horizontal. On the contrary, the MeOH/EG molar ratio does strongly affect the equilibrium DMT yield. As an example, if MeOH/EG is increased from 6.5 to 24, the equilibrium yield of DMT (i.e., reached when the dashed lines become horizontal) raises from 80 % to 92 % when the solvent to oligomers molar ratio is equal to 150.

Finally, the last parameter kept constant was the MeOH/EG molar ratio, set to 16, while ranging Solv/Olig from 1 to 200, and w_{cat} from 10^{-6} to 10^{-3}. The obtained results in terms of DMT yield reached after 90 min are shown in Fig. 9c, where the vertical red line highlights the region where Solv/Olig > 40, which is necessary to ensure homogeneous reaction conditions. When operating in homogeneous reaction conditions, the Solv/Olig molar ratio has no influence on the yield of DMT, as evident by the dashed lines. This means, for example, that operating at Solv/Olig molar ratio equal to 70 or 180 does not change the DMT produced in the system for any given w_{cat}. Moreover, it is confirmed that before reaching the equilibrium conditions, the yield of DMT increases when increasing the mass fraction of catalyst. For example, a yield of DMT greater than 92 % can be reached after 90 min using a mass fraction of catalyst equal to $1 \bullet 10^{-4}$, while only 60 % DMT yield can be obtained if the catalyst is reduced to $1 \bullet 10^{-5}$ after the same reaction time.

Finally, the concepts highlighted from the model predictions are better represented in Fig. 10, where the equilibrium DMT yield reached when varying the MeOH/EG molar ratio from 0 to 50 for different values of the Solv/Olig molar ratio (i.e., 25, 40, 50, 75, 100, 125, 150, 175, 200, and 300) is represented. The result of this last simulation confirms the influence of these two parameters on the equilibrium yield of DMT. Indeed, from Fig. 10, it is clear that the Solv/Olig molar ratio minimally affects the equilibrium yield of DMT, at least above a ratio equal to 40 for which homogeneous reaction conditions are ensured throughout the reaction. On the other hand, the value of the MeOH/EG molar ratio does strongly affect the equilibrium yield of DMT. Indeed, if MeOH/EG is increased from 0 to 15, the DMT yield at equilibrium does strongly increase from 0 % to 90 %. The slope of this curve decreases above MeOH/EG = 15, such that when this ratio is further increased up to 50, the equilibrium yield of DMT only reaches 96 %. Therefore, it is confirmed that the yield of DMT at equilibrium is mainly affected by the value of the MeOH/EG molar ratio, which should be carefully selected according to the minimum yield to DMT that can be accepted. As an example, a MeOH/EG molar ratio of at least 15 is required to reach an equilibrium yield to DMT of 90 %. When working below this value, it is never possible to reach this yield by any combination of the parameters w_{cat} and Solv/Olig.

4. Conclusions

In this work, the transesterification reaction of bis(2-hydroxyethyl) terephthalate (BHET) to dimethyl terephthalate (DMT) was systematically studied in order to shed light on the role of crucial process parameters like MeOH/EG, Solv/Olig and w_{cat} and in turn to guide the optimization of a process that, brought to industrial maturity, has the potential to push PET chemical recycling.

A detailed kinetic model of the reaction has been established and its parameters tuned by comparing the simulation results with experiments conducted at different reaction conditions. After this preliminary parameter tuning, the model allowed us to gather important information on the process conduction.

In particular, it has been demonstrated that the solvent to oligomers molar ratio has a minimal influence on the equilibrium yield to DMT, provided it is sufficiently high (>40) to prevent the DMT precipitation out of the reaction solution. Industrially, this means that the process can be conducted on concentrated feedstocks, which compresses the reaction volume and limits the demand for organic solvents. Conversely, the MeOH/EG molar ratio strongly affects the DMT equilibrium yield, and in order to get a sufficient DMT yield (for example, equal to 90 %), this

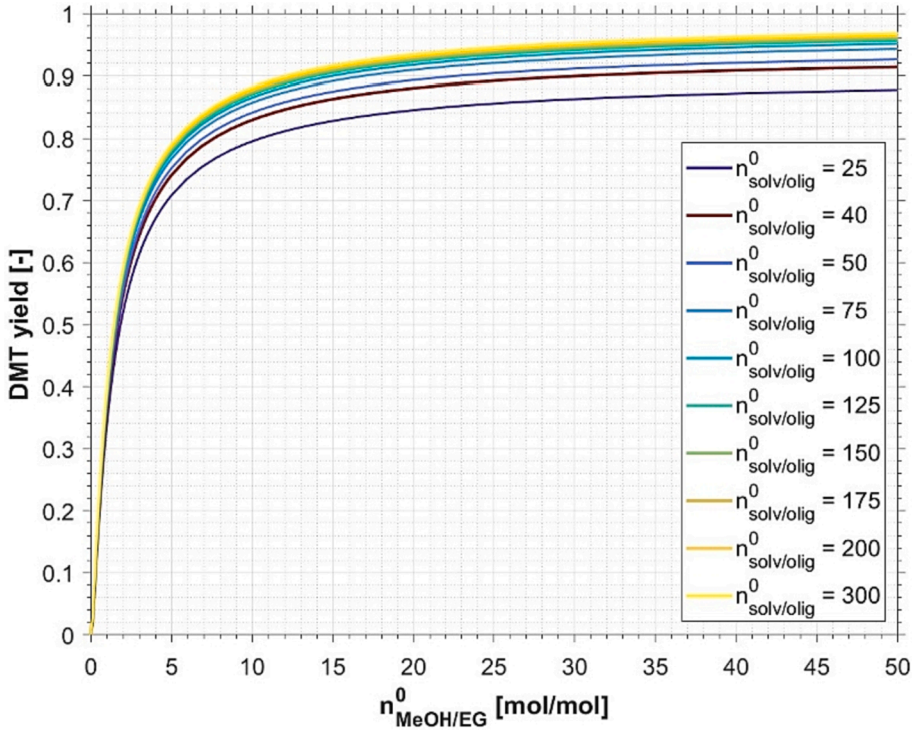

Fig. 10. DMT yield at equilibrium at different solvent to oligomers molar ratios by changing the methanol to ethylene glycol molar ratio.

ratio must be at least greater than 15. On the contrary, the mass fraction of catalyst determines the time needed to achieve the equilibrium, and a proper value can be selected in order to have a fast transesterification reaction. A catalyst mass fraction equal to $1 \bullet 10^{-4}$ allows to get a yield of DMT equal to 90 % after 90 min if using a MeOH/EG molar ratio equal to 15, and a solvent to oligomers molar ratio equal to 100. These last values for the three investigated parameters were considered to be satisfying both in terms of the obtained DMT yield and in terms of the amount of solvent to be used, in the framework of an industrial process where a solvent recycle loop can be easily implemented.

Author contribution

L.B.: Investigation, Data Curation, Writing – Original Draft; S.M.: Validation, Data Curation, Software; M.S.: Supervision, Writing – Review & Editing; D.M.: Funding Acquisition, Writing – Review & Editing.

Conflict of interest

The authors declare no conflict of interests.

CRediT authorship contribution statement

Lorenzo Brivio: Investigation, Data curation, Writing – original draft. **Serena Meini:** Validation, Data curation, Software. **Mattia Sponchioni:** Supervision, Writing – review & editing. **Davide Moscatelli:** Funding acquisition, Writing – review & editing.

Declaration of Competing Interest

The authors declare that they have no known competing financial interests or personal relationships that could have appeared to influence the work reported in this paper.

Data availability

Data will be made available on request.

Appendix A. Supplementary data

Electronic supplementary information is available at the publisher's website, reporting the external HPLC calibration for the different species involved in the process, the expression of the material balances for all the species, the results of the optimization with 4 values of α, and the simulations exploring the combination of two out of the three parameters at different reaction times. Supplementary data to this article can be found online at https://doi.org/10.1016/j.ces.2023.119466.

References

Abdi, H. Kendall Rank Correlation Coefficient. *The Concise Encyclopedia of Statistics* 278–281 (2008) doi:10.1007/978-0-387-32833-1_211.

Barnard, E., Rubio Arias, J. J. & Thielemans, W. Chemolytic depolymerisation of PET: A review. *Green Chem.* **23**, 3765–3789 (2021).

Besnoin, J.-M., Lei, G.D., Choi, K.Y., 1989. Melt transesterification of dimethyl terephthalate with ethylene glycol. AIChE J. 35, 1445–1456.

Brivio, L., Tollini, F., 2022. PET recycling: Review of the current available technologies and industrial perspectives. Adv. Chem. Eng. 60, 215–267.

Chai, T., Draxler, R.R., 2014. Root mean square error (RMSE) or mean absolute error (MAE)? -Arguments against avoiding RMSE in the literature. Geosci. Model Dev. 7, 1247–1250.

Chen, J., Chen, L., Cheng, W., 1999. Kinetics of glycolysis of polyethylene terephthalate with zinc catalyst. Polym. Int. 48, 885–888.

El-Mihoub, T.A., Hopgood, A.A., Nolle, L., Battersby, A., 2006. Hybrid Genetic Algorithms : A Review. Eng. Lett. 11, 124–137.

Espinosa, S., Bosch, E., Roses, M., 2000. Retention of ionizable compounds on HPLC. 5. pH scales and the retention of acids and bases with acetonitrile-water mobile phases. Anal. Chem. 72, 5193–5200.

Textile Exchange. Preferred Fiber & Materials: Market Report 2022. 1–118 (2022).

Fleckenstein, Dr. P. J. & Fleckenstein, P. J. Cyclic Polyethylene Furanoate Oligomers for Ring-Opening Polymerization. *A thesis submitted to attain the degree of DOCTOR OF SCIENCES of ETH ZURICH* (1988).

Geyer, B., Lorenz, G., Kandelbauer, A., 2016. Recycling of poly(ethylene terephthalate) – A review focusing on chemical methods. Express Polym. Lett. 10, 559–586.

Ghosal, K., Nayak, C., 2022. Recent advances in chemical recycling of polyethylene terephthalate waste into value added products for sustainable coating solutions-hope vs. hype. Mater. Adv. 3, 1974–1992.

Huang, J., Yan, D., Dong, H., Li, F., Lu, X., 2021. Removal of trace amount impurities in glycolytic monomer of polyethylene terephthalate by recrystallization. J. Environ. Chem. Eng. 9, 106277.

Jadhav, A.L., Malkar, R.S., Yadav, G.D., 2020. Zn-and Ti-Modified Hydrotalcites for Transesterification of Dimethyl Terephthalate with Ethylene Glycol: Effect of the Metal Oxide and Catalyst Synthesis Method. ACS Omega 5, 2088–2096.

Khoonkari, M., Haghighi, A.H., Sefidbakht, Y., Shekoohi, K., Ghaderian, A., 2015. Chemical recycling of PET wastes with different catalysts. Int. J. Polym. Sci. 2015.

Lin, C.-C., Baliga, S., 1986. A study on the polycondensation of bis-hydroxyethyl terephthalate. J. Appl. Polym. Sci. 31, 2483–2489.

López-Fonseca, R., Duque-Ingunza, I., de Rivas, B., Arnaiz, S., Gutiérrez-Ortiz, J.I., 2010. Chemical recycling of post-consumer PET wastes by glycolysis in the presence of metal salts. Polym. Degrad. Stab. 95, 1022–1028.

López-Fonseca, R., Duque-Ingunza, I., de Rivas, B., Flores-Giraldo, L., Gutiérrez-Ortiz, J. I., 2011. Kinetics of catalytic glycolysis of PET wastes with sodium carbonate. Chem. Eng. J. 168, 312–320.

Mandal, S., Dey, A., 2019. PET chemistry. Recycl. Polyethyl. Terephthalate Bottles 1–22. https://doi.org/10.1016/b978-0-12-811361-5.00001-8.

MiPol; Gr3n. Recycling polymeric materials via an alkaline hydrolysis depolymerization process: gr3n approach. https://www.milanpolymerdays.org/blog/recycling-polymeric-materials-via-an-alkaline-hydrolysis-depolymerization-process-gr3n-approach (2021).

Moscatelli, D. & Pelucchi, M. *Advances in chemical engineering: Towards circular economy: Recycling of solid plastic waste*. vol. 5 (2020).

Nikiema, J., Asiedu, Z., 2022. A review of the cost and effectiveness of solutions to address plastic pollution. Environ. Sci. Pollut. Res. 29, 24547–24573.

Nikles, D.E., Farahat, M.S., 2005. New motivation for the depolymerization products derived from poly(ethylene terephthalate) (PET) waste: A review. Macromol. Mater. Eng. 290, 13–30.

PackagingWorld. 2020 PET Recycling Rate Drops, While Demand for rPET Surges. (2021).

Padhan, R. K. & Sreeram, A. *Chemical Depolymerization of PET Bottles via Combined Chemolysis Methods. Recycling of Polyethylene Terephthalate Bottles* (Elsevier Inc., 2019). doi:10.1016/b978-0-12-811361-5.00007-9.

Pham, D.D., Cho, J., 2021. Low-energy catalytic methanolysis of poly (ethyleneterephthalate). Green Chem. 23, 511–525.

PlasticsEurope. Plastics the fact 2021. *Plastics Europe Market Research Group (PEMRG) and Conversio Market & Strategy GmbH.* (2021).

Ragaert, K., Delva, L., Van Geem, K., 2017. Mechanical and chemical recycling of solid plastic waste. Waste Manag. 69, 24–58.

Schyns, Z.O.G., Shaver, M.P., 2021. Mechanical recycling of packaging plastics: a review. Macromol. Rapid Commun. 42, 1–27.

Sheel, A. & Pant, D. *Chemical Depolymerization of PET Bottles via Glycolysis. Recycling of Polyethylene Terephthalate Bottles* (Elsevier Inc., 2019). doi:10.1016/b978-0-12-811361-5.00004-3.

Shojaei, B., Abtahi, M., Najafi, M., 2020. Chemical recycling of PET: A stepping-stone toward sustainability. Polym. Adv. Technol. 31, 2912–2938.

Sinha, V., Patel, M.R., Patel, J.V., 2010. Pet waste management by chemical recycling: A review. J. Polym. Environ. 18, 8–25.

Statista. *Demand for polyethylene terephthalate worldwide from 2010 to 2020, with a forecast for 2021 to 2030*. (2020).

Stratmann, F. *et al. Simulation of Micro-structure / Mechanism Relationships in Particle Deposition. Talbot, L. Thermophoresis-A Review. In Rarefied Gas Dynamics, Part I* vol. 31 https://pubs.acs.org/sharingguidelines (1992).

Tollini, F., Brivio, L., Innocenti, P., Sponchioni, M., Moscatelli, D., 2022. Influence of the catalytic system on the methanolysis of polyethylene terephthalate at mild conditions: A systematic investigation. Chem. Eng. Sci. 260, 117875.

Tomita, K. & Ida, H. *Studies on the formation of poly(ethylene terephthalate): 2. Rate of transesterification of dimethyl terephthalate with ethylene glycol.*

Tomita, K., Ida, H., 1973. Studies on the formation of poly(ethylene terephthalate): 2. Rate of transesterification of dimethyl terephthalate with ethylene glycol. Polymer (guildf) 14, 55–60.

Viana, M.E., Riul, A., Carvalho, G.M., Rubira, A.F., Muniz, E.C., 2011. Chemical recycling of PET by catalyzed glycolysis: Kinetics of the heterogeneous reaction. Chem. Eng. J. 173, 210–219.

Welle, F., 2011. Twenty years of PET bottle to bottle recycling - An overview. Resour. Conserv. Recycl. 55, 865–875.

Xin, J., et al., 2021. Progress in the catalytic glycolysis of polyethylene terephthalate. J. Environ. Manage. 296, 113267.

Zhang, H., Xia, Q., Yang, Y., Zhang, F., Zhang, G., 2013. Solubility of Dimethyl Terephthalate and Monomethyl Terephthalate in the methanol aqueous solution and its application to recycle Monomethyl Terephthalate from crude Dimethyl Terephthalate. Ind. Eng. Chem. Res.